

Photoemission study of valence fluctuation in YbCu₂

A. Fujimori

National Institute for Research in Inorganic Materials, Sakura-mura, Niihari-gun, Ibaraki 305, Japan

T. Shimizu and H. Yasuoka

The Institute for Solid State Physics, The University of Tokyo, Roppongi, Minato-ku, Tokyo 106, Japan

(Received 27 October 1986)

Mixed-valence YbCu₂ has been studied by x-ray and ultraviolet photoemission spectroscopy (XPS and UPS). UPS results reveal a bulk divalent ($4f^{14} \rightarrow 4f^{13}$) peak ~ 0.3 eV below the Fermi level, and a valence of 2.2 is deduced from XPS. These values are compared with the ground-state magnetic susceptibility, the specific heat, and the magnetic relaxation rate of $4f$ electrons by using the results of the degenerate impurity Anderson model. The $4f-5d$ -conduction-band hybridization is suggested to be more important than the $4f-sp$ -conduction-band hybridization.

I. INTRODUCTION

There has been considerable interest in valence-fluctuation phenomena in rare-earth compounds.¹ Anomalous behaviors of magnetic, electrical, thermal, and structural properties in these compounds have been attributed to a near degeneracy of two electronic configurations, $4f^n$ and $4f^{n+1}$, of the rare-earth ion in the configuration-based picture.² This has been directly proved by photoemission experiments, which show two sets of final-state multiplets, $4f^{n-1}$ and $4f^n$, in the valence-band region with the lowest-binding-energy component of the $4f^n$ multiplet located close to the Fermi level (E_F).³ However, there has been controversy on the relevance of such a high-energy probe to investigation of the low-energy properties and on the relationship between information obtained by photoemission and low-energy experiments.

In particular, for Ce and its compounds, the valence determined by photoemission or x-ray absorption is generally much lower than that estimated from low-energy experiments.^{4,5} The discrepancy is attributed to large $4f$ -valence (conduction) -band hybridization $\Delta \equiv \pi\rho V^2$ of the order of 0.1 eV,⁶ where ρ and V are the conduction-band density of states (DOS) and the $4f$ -conduction-band hybridization matrix element, respectively, evaluated at E_F , while much smaller values $\Delta \simeq 0.001-0.01$ eV have been assumed so far. Almost all metallic Ce compounds are found to be in the so-called Kondo regime, i.e., the number of $4f$ electrons n_f is greater than ~ 0.8 but, as far as low-energy properties such as magnetic susceptibilities are concerned, some of them appear to be of mixed valence or tetravalent due to strong $4f$ -valence-band hybridization. Recent theoretical studies on the degenerate impurity Anderson model have demonstrated that this situation can be understood in terms of the universal aspect of the $4f$ DOS as shown in Fig. 1. Due to the large $4f$ -orbital degeneracy N_f , the $4f^0 \rightarrow 4f^1$ spectral weight shows a peak at ϵ_f above E_F and the temperature-dependent physical properties scale with a characteristic temperature⁷ $T_0 \approx \epsilon_f/k$. In the Kondo regime [Fig. 1(a)] the bare $4f$ level ϵ_f^0 is well

below E_F and T_0 is equal to the Kondo temperature T_K , while in the mixed-valence regime [Fig. 1(b)] ϵ_f^0 is near E_F or ϵ_f .⁷ The $4f^1 \rightarrow 4f^0$ spectral weight in the Kondo regime has a double-peak structure, one at E_F and the other near ϵ_f^0 (a few eV below E_F) as has been observed by photoemission spectroscopy.⁸ The latter deeper peak disappears in the mixed-valence regime ($n_f \ll 0.8$),⁹ though this situation rarely occurs in Ce systems.

In mixed-valence Yb compounds, charge fluctuation takes place between divalent ($4f^{14}$) and trivalent ($4f^{13}$) configurations, and therefore photoemission can probe the

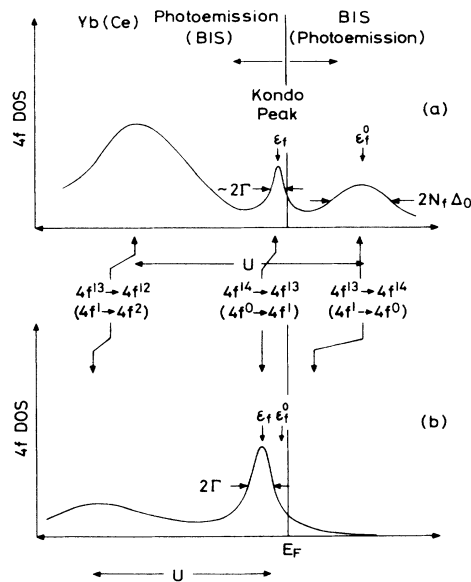


FIG. 1. Schematic representation of the $4f$ spectral density of states for Yb (Ce) compounds in (a) the Kondo and (b) the mixed-valence regimes. The spin-orbit splitting of the $4f^{13}$ ($4f^1$) final states as well as the multiplet structure of the $4f^{12}$ ($4f^2$) final states are not shown. ϵ_f , $4f$ peak position; ϵ_f^0 , bare $4f$ -level position.

$4f$ DOS corresponding to the $4f^0 \rightarrow 4f^1$ spectral weight of Ce systems as can be seen from Fig. 1. Thus high-resolution photoemission studies of Yb compounds spanning a wide range of valences would reveal systematic changes in the $4f$ -derived DOS and their relevance to the low-energy properties, since the unoccupied $4f$ DOS in Ce systems cannot be studied with comparable resolution because of the limitation of the current bremsstrahlung isochromat spectroscopy (BIS) technique.

In this paper, we report results of a photoemission study on YbCu_2 which has been reported to be mixed valent, with a valence of $\nu = 2.4\text{--}2.5$ according to magnetic¹⁰ and lattice-constant¹¹ measurements. When interpreting the experimental results, we will make use of the local Fermi-liquid (LFL) theory of Newns and Hewson¹² and the degenerate impurity Anderson-model results by Kuramoto *et al.*^{9,13} and by Ramakrishnan and Sur.¹⁴ In most previous photoemission works on mixed-valence systems, the lowest-energy $4f^n$ multiplet has been assumed at E_F (Ref. 3), or, even if it is noticeably shifted from E_F , the shift has not been paid attention to or has been attributed to a final-state effect in the photoemission process (relaxation or screening effect).^{15,16} However, it should be noted that in the mixed-valence regime $kT_0 = \epsilon_f^0$ can be of the order of ~ 0.1 eV and a $4f^{14} \rightarrow 4f^{13}$ peak may be observed distinctly below E_F . In fact, parameters we have deduced from experiment—the number of $4f$ holes $n_f \sim 0.2$, and the photoemission peak position relative to E_F , $\epsilon_f \sim 0.3$ eV—will be shown to be quantitatively consistent with the magnetic and thermal properties predicted by the Anderson model and the LFL theory.

II. EXPERIMENT

Samples were prepared by the arc-melting method, and were checked to be single phases by x-ray diffraction. Spectra were taken with a spectrometer equipped with a Mg $K\alpha$ radiation source and a He resonance lamp and photoelectrons were collected with a double-pass cylindrical mirror analyzer. The base pressure of the spectrometer was $\sim 5 \times 10^{-11}$ Torr. The surface was cleaned *in situ* by scraping with a diamond file. The cleaning was done periodically in order to keep the oxygen contamination below the detectability limit [as monitored by the O $1s$ peak in x-ray photoemission spectroscopy (XPS) and the O $2p$ emission in ultraviolet photoemission spectroscopy (UPS)]. The energy resolution of UPS was 0.18 eV as determined from the Fermi edge of Cu metal, out of which ~ 0.05 eV is due to the thermal distribution of electrons at room temperature.

III. RESULTS

Figure 2 shows He I ($h\nu = 21.2$ eV) and He II ($h\nu = 40.8$ eV) UPS and XPS ($h\nu = 1253.6$ eV) spectra in the valence-band region. The emission features extending from E_F to ~ 2.5 eV below it become intense with increasing photon energy and are attributed to $4f^{14} \rightarrow 4f^{13}$ emission from divalent Yb superposed on the fairly smooth Yb $5d$ band emission. Below this region (at 2–5 eV) the Cu $3d$ band is located, and at 5–13 eV

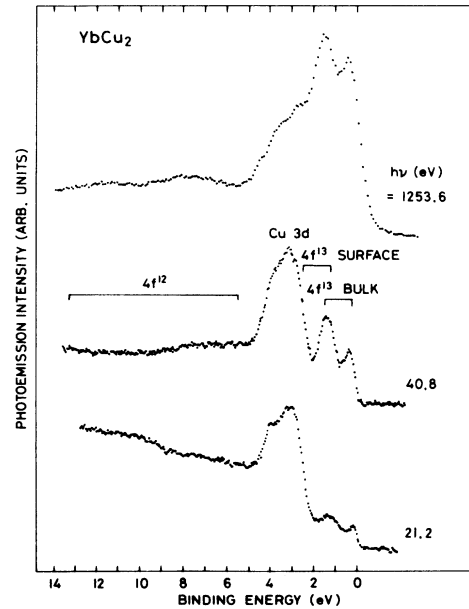


FIG. 2. XPS and UPS spectra of YbCu_2 in the valence-band region.

$4f^{13} \rightarrow 4f^{12}$ emission from trivalent Yb is identified. Figure 3 shows the $4f^{13}$ final-state region of the He II spectrum on an expanded energy scale. The $4f^{13}$ features consist of two overlapping spin-orbit doublets, for each of which one can identify $^2F_{7/2}$ and $^2F_{5/2}$ peaks separated by about 1.3 eV. The $^2F_{7/2}$ peak of the lower-binding-energy doublet is located close to E_F as expected from the bulk valence-fluctuation behavior. On the surfaces of mixed-valence Yb compounds, Yb atoms are converted to divalent,^{15,16} and $4f^{13}$ peaks arising from the surface divalent Yb atoms are shifted to higher binding energies relative to bulk $4f^{13}$ peaks. The higher-binding-energy $4f^{13}$ doublet is thus attributed to the surface divalent Yb. This emission was in fact found suppressed by an exposure of ~ 1 L O_2 , confirming its surface origin.

The bulk $4f^{13}$ peaks were fitted to an asymmetric line shape given by Mahan¹⁷ (with a cutoff energy of $\xi = 6$ eV) convoluted with Gaussian and Lorentzian broadening functions representing, respectively, the instrumental and lifetime broadening effects. In order to evaluate contributions from the Cu and Yb $5d$ bands, the He II spectrum of isostructural LuCu_2 , for which the $4f$ emission is below the Cu $3d$ band, was measured. The Lu $5d$ band was fitted to a step function with a step at E_F plus a Gaussian peak just below E_F , and the Cu $3d$ band to two Gaussians as is shown in Fig. 3. In going from LuCu_2 to YbCu_2 , the position of E_F within the $5d$ band was shifted by 0.3 eV downward in order to represent the decrease in the conduction electron number, and the Cu $3d$ band was allowed to be narrowed (by 15%) because of the increased Cu-Cu distance. The surface $4f^{13}$ peaks were assumed to be symmetric as they have been found to be highly symmetric in most Yb compounds including Yb metal.^{15,16,18,19} Integral backgrounds were assumed except for the surface

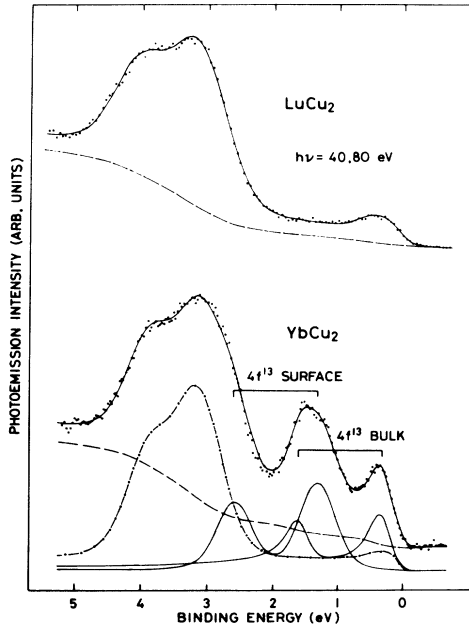


FIG. 3. He II UPS spectrum of YbCu₂ (dots) in the $4f^{14} \rightarrow 4f^{13}$ region fitted to a superposition of the bulk and surface $4f^{13}$ spin-orbit doublets, the Cu 3d and Yb 5d bands (dot-dashed curves), and the integral background (dashed curve). The $4f^{13}$ doublet due to divalent surface Yb atoms appears at ~ 1.0 eV higher binding energies than the bulk one. The He II spectrum of LuCu₂ is also shown.

$4f^{13}$ peaks, for which such a background is expected to be weak since photoelectrons from surface atoms escape from the surface before traveling in the bulk. The energy positions, intensities, Gaussian and lifetime widths, singularity index, and background intensities were treated as adjustable parameters. The spin-orbit splittings of the bulk and surface doublets were set to be identical and the statistical ratio 4:3 was assumed for the intensity ratio. As for the $4f^{12}$ emission, the same singularity index as that of the bulk $4f^{13}$ peaks was used. The $4f^{12}$ multiplet structure was taken from a calculation by Gerken *et al.*,²⁰ but we allowed for a uniform expansion of the energy scale by 1.16. Since XPS does not have sufficient resolution to resolve the surface $4f^{13}$ peaks from the bulk one,

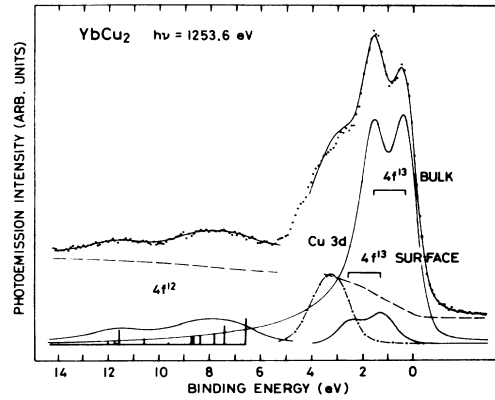


FIG. 4. XPS spectrum of YbCu₂ (dots) in the valence-band region fitted to a superposition of the $4f^{12}$ multiplet, the bulk and surface $4f^{13}$ spin-orbit doublets, the Cu 3d band (dot-dashed curve), and the integral background (dashed curve).

the energies of the bulk and surface $4f^{13}$ peaks and the singularity index were fixed at the values obtained for the He II spectrum with appropriately increased Gaussian and lifetime widths.

Resulting fits are shown in Fig. 3 for He II UPS and in Fig. 4 for XPS, and the parameters are shown in Table I. The Gaussian full width at half maximum (FWHM) of these peaks is similar to the broadening of the Cu metal Fermi edge, whereas that of the surface $4f^{13}$ peaks is considerably larger than this, suggesting the presence of inequivalent atomic sites on the surface. It should be noted that we could fit the $4f^{13}$ emission without assuming a second surface $4f^{13}$ doublet located between the bulk and surface components as has been found for YbAl₂.^{15,19}

IV. DISCUSSION

From the valence 2.2 thus obtained, YbCu₂ is found to be in the strongly mixed-valence regime. According to the results of the self-consistent perturbation calculations on the degenerate impurity Anderson model by Kuramoto and Kojima,⁹ only the ${}^2F_{7/2}$ peak (ϵ_f below E_F) is near E_F and can be involved in the low-energy properties. The $4f^{13} \rightarrow 4f^{12}$ spectral weight (more than ~ 7 eV below E_F by the f - f Coulomb correlation) and the $4f^{14} \rightarrow 4f^{13} {}^2F_{5/2}$ peak (~ 1.5 eV below E_F) do not contribute to the low-

TABLE I. The $4f$ -hole number n_f , the binding energy of the $4f^{13} {}^2F_{7/2}$ peak ϵ_f , the singularity index α , and the Lorentzian and Gaussian FWHM's (2Γ and $2G$) for the $4f$ photoemission peaks in YbCu₂.

	n_f	ϵ_f	α	2Γ	$2G$
$4f^{13}$ bulk	0.18 ± 0.03	0.30 ± 0.05	$0.25^{+0.05}_{-0.15}$	0.16 ± 0.05	0.24 ± 0.05
$4f^{13}$ surface		1.27 ± 0.05	0.0	0.16 ± 0.05^a	0.61 ± 0.08
$4f^{12}$			$0.25^{+0.05}_{-0.15}{}^a$	1.3^b	0.85^b

^aAssumed to be the same as that of the bulk $4f^{13}$ peaks.

^bThese values should be corrected for the larger width of the x-ray source and the larger analyzer pass energy used for the XPS measurement by $2\Gamma \sim 0.3$ eV and $2G \sim 0.5$ eV, when compared with the $4f^{13}$ peaks.

energy properties. A spin-orbit sideband in the $4f^{13} \rightarrow 4f^{14}$ spectral weight which appears ~ 1.3 eV above E_F as predicted for photoemission in Ce compounds^{7,21} (not shown in Fig. 1) can also be ignored. Then the relevant $4f$ DOS is essentially a single peak, which is a symmetric Lorentzian as assumed in the LFL theory¹² or derived by the Anderson-model calculation in the mixed-valence regime.^{13,14} Thus various relations given by these theories between n_f , ε_f , the $4f$ -level width Γ , the orbital degeneracy N_f (equal to 8 for a ${}^2F_{7/2}$ state), the ground-state magnetic susceptibility $\chi(0)$, the coefficient of the linear specific-heat term γ , etc., can be tested to see whether the photoemission results are relevantly related to the low-energy properties.

Kuramoto and Müller-Hartmann,¹³ Ramakrishnan and Sur,¹⁴ and (in an approximate form) Newns and Hewson¹² have indicated that $\chi(0)$ can be given in terms of n_f and ε_f as

$$\chi(0) = kCn_f/\varepsilon_f, \quad (1)$$

where C is the Curie constant of the Yb^{3+} ion. Equation (1) combined with the LFL relation,¹² $\chi(0)/\gamma = [g^2\mu_B^2 J(J+1)]/[\pi^2 k^2]$, gives

$$\gamma = \pi^2 k^2 n_f / 3\varepsilon_f. \quad (2)$$

The magnetic relaxation rate of $4f$ electrons, $\Gamma_M = \chi(0)[\lim_{\omega \rightarrow 0} \text{Im}\chi(\omega)/\omega]^{-1}$, is given by the Korringa relation¹³

$$\Gamma_M = (N_f/\pi)(\varepsilon_f/n_f). \quad (3)$$

In Table II, $\chi(0)$, γ , and Γ_M calculated by using Eqs. (1)–(3) and ε_f and n_f obtained in the present work are listed and compared with experimental values. There one can see that the calculated $\chi(0)$ is in reasonable agreement with the experimental value.²² A possible valence change between $T=0$ and room temperature would be negligible because for YbAl_2 the valence changes by at most ≤ 0.1 between $T=100$ K and room temperature,^{22,23} and because the temperature dependence would be much weaker for YbCu_2 as judged from the flat χ - T curves.¹⁰ As for γ , the calculated value is only 20% of the experimental value.²² This discrepancy would largely be attributed to

contributions from $5d$ conduction electrons at E_F , as γ has been reported to be as large as $8 \text{ mJ K}^{-2} \text{ mol}^{-1}$ for LaCu_6 (Ref. 24) and $3\text{--}8 \text{ mJ K}^{-2} \text{ mol}^{-1}$ for Yb metal (Ref. 25). A significant discrepancy exists between the calculated Γ_M value and that obtained by the Yb NMR study.²⁶ As there is no such discrepancy for YbAl_2 whose valence is 2.4 (Ref. 15) (Table II), and since the spin-lattice relaxation rate $1/T_1$ and the Knight shift K of the Yb nucleus seem to satisfy the exact the Fermi-liquid relation,¹³ $T_1TK^2 = 2.29$, for both compounds [2.6 for YbCu_2 (Ref. 26) and 2.1 for YbAl_2 (Ref. 27)], the discrepancy might be traced to the inaccuracy of the approximate form (3) in the strongly mixed-valence regime.

Next, relations between n_f , ε_f , and Γ are discussed. Kuramoto and Müller-Hartmann¹³ have given

$$n_f = \Delta / [\Delta + (\pi/N_f)\varepsilon_f]. \quad (4)$$

Δ ($\equiv \pi\rho V^2$), which represents the $4f$ -conduction-band hybridization strength, is equal to the Lorentzian width Γ in the strongly mixed-valence regime, though in general Δ is greater than Γ . Using Eq. (4), $\varepsilon_f = 0.30$ eV and $n_f = 0.18$ lead to $2\Gamma \approx 2\Delta = 0.05 \pm 0.01$ eV. Experimentally we have obtained $2\Gamma = 0.16 \pm 0.05$ eV, which is significantly larger than this estimate. Further, the $4f^{13}F_{7/2}$ peak is highly asymmetric ($\alpha \sim 0.2$), whereas the Anderson-model theoretical calculations¹³ have shown that the peak is very close to a symmetric Lorentzian in the strongly mixed-valence regime. These discrepancies between theory and experiment are due to Coulomb interaction between the conduction electrons and the $4f$ hole, which is not explicitly considered in the Anderson model. The high asymmetry arises from the Fermi-edge singularity due to excitations of a large number of low-energy electron-hole pairs as in core-level photoemission spectroscopy.²⁸ The $4f$ -hole-conduction-electron Coulomb interaction also leads to the Auger decay of the $4f$ hole and consequently the large lifetime width as in the case of core-level XPS.²⁹ These Coulomb interaction effects are expected to become more important in going from the Kondo to mixed-valence regimes. Namely, in the divalent limit a localized $4f^{13}$ final state is an impurity with a positive unit charge embedded in the $4f^{14}$ host

TABLE II. The ground-state magnetic susceptibility $\chi(0)$, the linear specific-heat coefficient γ , and the magnetic relaxation rate Γ_M of YbCu_2 calculated from n_f and ε_f by using the analytical expressions of the degenerate Anderson model given by Kuramoto and Müller-Hartmann (Ref. 13), compared with experiment. The same quantities for YbAl_2 are also given.

	$\chi(0)$ ($10^{-3} \text{ emu mol}^{-1}$)	γ ($\text{mJ K}^{-2} \text{ mol}^{-1}$)	Γ_M (10^4 K)
YbCu_2 Calc.	0.13 ± 0.03	1.4 ± 0.3	4.9 ± 1.2
Expt.	0.16 ± 0.03^a	6.8 ± 0.5^a	3.3^b
YbAl_2 Calc. ^c	0.36 ± 0.10	3.9 ± 1.0	1.8 ± 0.5
Expt.	0.35 ± 0.04^a	16.8^a	1.6^d

^aReference 22. $\chi(0)$ has been corrected for the $5d$ -conduction-electron contribution, while γ has not. For YbAl_2 , $\chi(0)$ of LuAl_2 measured by us is used as the conduction-electron contribution.

^bReference 26.

^cCalculated using $n_f = 0.4$ and $\varepsilon_f = 0.24$ eV given in Ref. 15.

^dReference 27.

and behaves like a core hole, whereas in the Kondo limit a $4f^{13}$ final state is an impurity with only a small fraction of the unit charge in the almost $4f^{13}$ -like host. Thus we suspect that in the mixed-valence regime the $4f$ DOS deviates appreciably from that given by the original Anderson model. The disagreement between theory and experiment for γ and Γ_M might be attributed to these effects, but their importance has not been evaluated so far.

The $4f$ -conduction-band hybridization Δ is known to play an essential role in valence fluctuation phenomena, but it has not yet been elucidated what factors determine Δ in real systems. The systematics of the dependence of Δ on the chemical and structural environment is important since, according to Eq. (4), the valence, or n_f , is determined by ϵ_f and Δ . It has been argued that ϵ_f is largely determined by the electronegativity of the partner element, as it determines the position of E_F , or the work function.³⁰ On the other hand, relatively little is known about the nature of the $4f$ -conduction-band hybridization. We compare the YbCu₂ and YbAl₂ cases where Yb $5d$ and free-electron-like Cu $4sp$ or Al $3sp$ states interact with the $4f$ level. (Hybridization between $4f$ and Cu $3d$ would be negligible because the Cu $3d$ band is located 2–5 eV below $4f$ which is much larger than $2\Delta \sim 0.05$ eV.) As for YbAl₂, using Eq. (4) and ϵ_f and n_f given by Kaindl *et al.*¹⁵ one obtains $2\Delta = 0.13 \pm 0.02$ eV, which is larger than that of YbCu₂ by a factor of ~ 2.5 . The Yb-Yb distance is smaller for YbAl₂ (3.4 Å) than for YbCu₂ (~ 3.6 Å) with the same coordination number (equal to 4), whereas the Yb atom is coordinated by 12 Al atoms at a distance of 3.3 Å in YbAl₂ and by the same number of Cu atoms at a distance of 3.0–3.2 Å in YbCu₂.^{11,31} Thus there is a correlation between Δ and the Yb-Yb distance but not between Δ and the Yb-partner-atom distance. Therefore, it seems reasonable to assume that Δ is predominantly determined by the $4f$ - $5d$ hybridization rather than the $4f$ - sp hybridization. Indeed, a recent perturbed γ -ray angular correlation study has shown that the $4f$ local moment of light rare-earth atoms implanted in a d -band metal host is more unstable than that of atoms implanted in an sp metal host.³² On the other hand, the $4f$ - sp hybridization might also explain the difference in Δ by the difference in ρ through $\Delta = \pi\rho V^2$. Namely, the sp DOS at E_F would be higher for YbAl₂ than for YbCu₂, because the sp band is more populated for trivalent Al than for monovalent Cu. However, the sp

DOS at E_F is not critically dependent on the number of sp electrons: In going from a monovalent to a trivalent free-electron metal, the DOS increases only by a factor of 1.44 as compared to the derived factor of ~ 2.5 for Δ . The correlation between the Yb-Yb distance and Δ would not, of course, suggest direct or indirect interaction between neighboring $4f$ orbitals, since it is well established that valence-fluctuation phenomena in these Yb compounds are single- $4f$ -ion properties.^{10,11,33}

V. CONCLUSION

We have studied the occupied $4f$ DOS in the mixed-valence compound YbCu₂ by photoemission spectroscopy. It is demonstrated within the degenerate impurity Anderson model or the LFL theory that the spectra are consistent with low-energy properties such as $\chi(0)$ and γ . However, the lifetime width and the asymmetry of the $4f^{13}$ peaks are considerably larger than those predicted by these theories because of the Auger decay of the $4f$ hole and the Fermi-edge singularity effect. It is suggested that the $4f$ -conduction-band hybridization is dominated by $4f$ - $5d$ interaction between neighboring Yb atoms rather than $4f$ - sp interaction.

Here it is important to note that the $4f$ -conduction-band hybridization strength $\Delta = \pi\rho V^2$ itself is smaller in Yb compounds than in Ce compounds only by a factor of the order of 2–5. The apparently strong hybridization effect in the photoemission spectra of Ce compounds is mainly due to the fact that, while a relevant energy scale for photoemission in Yb compounds is Δ , it is $N_f\Delta$ ($N_f = 14$) for Ce compounds. This is because 14 empty $4f$ orbitals are available for the screening of a photoproduced $4f$ hole in Ce, while only one is involved in Yb. In the case of BIS of Yb compounds, on the other hand, one expects to see a strong hybridization effect, i.e., a double-peak $4f$ structure as in the photoemission spectra of Ce compounds [see Fig. 1(a) and Ref. 34].

ACKNOWLEDGMENTS

We would like to thank Y. Kuramoto and S.-J. Oh for useful discussions and M. Sekita for technical support. One of us (A.F.) is grateful to S. Suga for drawing his attention to the present problem.

¹For review, see J. M. Lawrence, P. S. Riseborough, and R. D. Parks, *Rep. Prog. Phys.* **44**, 1 (1981); C. M. Varma, *Rev. Mod. Phys.* **48**, 219 (1976).

²L. L. Hirst, *Phys. Kondens. Mater.* **11**, 255 (1970); *J. Phys. Chem. Solids* **35**, 1285 (1974).

³M. Campagna, G. K. Wertheim, and Y. Baer, in *Photoemission in Solids II*, edited by L. Ley and M. Cardona (Springer-Verlag, Berlin, 1978), p. 217.

⁴For example, F. U. Hillebrecht and J. C. Fuggle, *Phys. Rev. B* **25**, 3550 (1982).

⁵K. R. Bauchspiess, W. Boksich, E. Holland-Moritz, H. Launois, R. Pott, and D. Wohlleben, in *Valence Fluctuations in Solids*,

edited by L. M. Falicov, W. Hanke, and M. B. Maple (North-Holland, Amsterdam, 1981), p. 417.

⁶J. C. Fuggle, F. U. Hillebrecht, Z. Zolnierok, R. Lässer, Ch. Freiburg, O. Gunnarsson, and K. Schönhammer, *Phys. Rev. B* **27**, 7330 (1983); A. Fujimori, *ibid.* **28**, 4489 (1983).

⁷N. E. Bickers, D. L. Cox, and J. W. Wilkins, *Phys. Rev. Lett.* **54**, 230 (1985).

⁸R. D. Parks, N. Mårtensson, and B. Reihl, in *Valence Instabilities*, edited by P. Wachter and H. Boppart (North-Holland, Amsterdam, 1982), p. 239; J. W. Allen, S.-J. Oh, M. B. Maple, and M. S. Torikachvili, *Phys. Rev. B* **28**, 5347 (1983).

⁹Y. Kuramoto and H. Kojima, *Z. Phys.* **57**, 95 (1984).

- ¹⁰J. C. P. Klasse, W. C. M. Mattens, F. R. de Boer, and P. F. de Châtel, *Physica* **86-88B**, 234 (1977).
- ¹¹D. Debray, *J. Less-Common Met.* **30**, 237 (1973); E. Graz, E. Bauer, B. Barbara, S. Zemir, F. Steglich, C. D. Bredl, and W. Lieke, *J. Phys. F* **15**, 1975 (1985).
- ¹²D. M. News and A. C. Hewson, *J. Phys. F* **10**, 2429 (1980).
- ¹³Y. Kuramoto and E. Müller-Hartmann, *J. Magn. Magn. Mater.* **52**, 122 (1985).
- ¹⁴T. V. Ramakrishnan and K. Sur, *Phys. Rev. B* **26**, 1798 (1982).
- ¹⁵G. Kaindl, B. Reihl, D. E. Eastman, P. A. Pollak, N. Mårtensson, B. Barbara, T. Penny, and T. S. Plaskett, *Solid State Commun.* **41**, 157 (1982).
- ¹⁶M. Domke, C. Laubschat, E. V. Sampathkumaran, M. Prietsch, T. Mandel, and G. Kaindl, *Phys. Rev. B* **32**, 8002 (1985).
- ¹⁷G. D. Mahan, *Phys. Rev. B* **11**, 4814 (1975).
- ¹⁸S. F. Alvarado, M. Campagna, and W. Gudat, *J. Electron Spectrosc. Relat. Phenom.* **18**, 13 (1980); M. H. Hecht, A. J. Viescas, I. Lindau, J. W. Allen, and L. I. Johansson, *ibid.* **34**, 343 (1984).
- ¹⁹R. Nyholm, I. Chorkendorff, and J. Schmidt-May, *Surf. Sci.* **143**, 177 (1984).
- ²⁰F. Gerken, *J. Phys. F* **13**, 703 (1983).
- ²¹O. Sakai, H. Takahashi, M. Takeshige, and T. Kasuya, *Solid State Commun.* **52**, 997 (1984).
- ²²J. C. P. Klasse, F. R. de Boer, and P. F. de Châtel, *Physica* **106B**, 178 (1981).
- ²³S.-J. Oh, J. W. Allen, M. S. Torikachvili, and M. B. Maple, *J. Magn. Magn. Mater.* **52**, 183 (1985).
- ²⁴T. Fujita, K. Satoh, Y. Ōnuki, and T. Komatsubara, *J. Magn. Magn. Mater.* **47/48**, 66 (1985).
- ²⁵E. Bucher, P. H. Schmidt, A. Jayaraman, K. Andres, J. P. Maita, K. Nassau, and P. D. Dernier, *Phys. Rev. B* **2**, 3911 (1970).
- ²⁶T. Shimizu, M. Takigawa, and H. Yasuoka (unpublished).
- ²⁷T. Shimizu, M. Takigawa, H. Yasuoka, and J. H. Wernick, *J. Magn. Magn. Mater.* **52**, 187 (1985).
- ²⁸G. K. Wertheim and P. H. Citrin, in *Photoemission in Solids I*, edited by M. Cardona and L. Ley (Springer-Verlag, Berlin, 1978), p. 197.
- ²⁹E. J. McGuire, *Phys. Rev. A* **19**, 1840 (1974); **13**, 1288 (1976).
- ³⁰G. K. Wertheim, J. H. Wernick, and G. Crecelius, *Phys. Rev. B* **18**, 875 (1978). In this reference, YbCu₂ is regarded as divalent and the 4*f*¹² feature has been identified as due to Yb oxide contamination. However, in the present study, at least ~80% of the 4*f*¹² signal is intrinsic considering the low oxygen contamination level.
- ³¹A. Iandelli and A. Palenzona, *J. Less-Common Met.* **29**, 293 (1972).
- ³²L. Buermann, H. J. Barth, K. H. Biedermann, M. Luszik-Bhadra, and D. Riegel, *Phys. Rev. Lett.* **56**, 492 (1986).
- ³³W. C. M. Mattens, P. F. de Châtel, A. C. Moleman, and F. R. de Boer, *Physica* **96B**, 138 (1979).
- ³⁴S.-J. Oh, S. Suga, A. Kakizaki, M. Taniguchi, T. Ishii, J.-S. Kang, J. W. Allen, O. Gunnarsson, N. Christensen, A. Fujimori, T. Suzuki, T. Kasuya, T. Miyahara, H. Kato, K. Schönhammer, M. S. Torikachvili, and M. B. Maple (unpublished).